Available online at www.sciencedirect.com
ScienceDirect
Biochemical and Biophysical Research Communications 366 (2008) 48–53
BBRC
www.elsevier.com/locate/ybbrc

Comparative effects of sodium pyrithione evoked intracellular calcium elevation in rodent and primate ventral horn motor neurons

Ronald J. Knox [a,1], Kim L. Keen [c], Laurelee Luchansky [c], Ei Terasawa [c], Hugh Freyer [a], Steven J. Barbee [b], Leonard K. Kaczmarek [a,*]

[a] *Department of Pharmacology, Yale University School of Medicine, 333 Cedar Street, New Haven, CT 06520-8066, USA*
[b] *Arch Chemicals Inc., Department of Regulatory Affairs and Toxicology, Cheshire, CT 06410, USA*
[c] *Wisconsin National Primate Center, University of Wisconsin, Madison, WI, USA*

Received 14 November 2007

Abstract

Oral administration of sodium pyrithione (NaP) causes hindlimb weakness in rodents, but not in primates. Previous work using *Aplysia* neurons has demonstrated that NaP produces a persistent influx of Ca^{2+} ions across the plasma membrane. To determine whether this also occurs in mammalian neurons and whether this could underlie the inter-species difference between rodents and primates, we have tested the effects of NaP on intracellular Ca^{2+} levels ($[Ca^{2+}]_i$) in rat and monkey motor neurons *in vitro*. Motor neurons present in spinal cord slices from rhesus monkey embryos (E37 and 56) and from rat E16 were dissected and cultured on glass coverslips. Following 2 weeks (rhesus) or 2–3 days (rat) in culture, neurons were loaded with fura-PE3/AM, and examined for $[Ca^{2+}]_i$ changes in response to NaP. Rhesus motor neurons were identified by immunostaining for Islet-1 (MN specific antigen) and neuron specific enolase (NSE). Motor neurons from both species exhibited dose-dependent NaP-evoked increases in $[Ca^{2+}]_i$ However, the dose–response curve for the Rhesus motor neurons was significantly shifted to the right of the rat dose–response curve, whereas the overall amplitude of the Ca^{2+} rise was similar in both species. As shown previously for the *Aplysia* neurons, the action of NaP is attenuated by SKF 96365, an inhibitor of store-operated calcium entry. In contrast the action of NaP is unaffected by nifedipine and tetrodotoxin, blockers of voltage-dependent Ca^{2+} and Na^+ channels, respectively, or by ouabain, an inhibitor of the plasma membrane Na^+/K^+ ATPase. Our results indicate that the NaP-induced increase in $[Ca^{2+}]_i$ is conserved across species and suggest that the toxicological sensitivity of rodent over primate to pyrithione could be due to the enhanced sensitivity of rodent motor neurons to NaP-evoked intracellular Ca^{2+} elevation.

Keywords: Sodium pyrithione; Calcium channels; Mammalian motor neurons

Sodium pyrithione (*N*-hydroxypyridine-2-thione) is a broad-spectrum fungistatic and antimicrobial agent that is the active ingredient of certain antidandruff shampoos and a common additive in sealants, adhesives, aerosols, and marine anti-fouling paints. It is usually administered as sodium, zinc, copper, or magnesium sulfate salt. When administered *in vivo* to rodents, pyrythiones cause hindlimb weakness. This reversible neurotoxicity in rodents is associated with the failure of synaptic transmission at neuromuscular junctions and with biochemical and histopathological changes in peripheral motor nerves and skeletal muscles [1,2].

Interestingly, although species other than rodents are also sensitive to the actions of pyrithiones [3,4], primates appear to be relatively insensitive as hindlimb weakness has not been observed in primates. For example, repeated exposure of zinc pyrithione (ZnPt) to rats has been shown to reduce the rate of axoplasmic transport and to result in the accumulation of tubulovesicular profiles at the distal nerve terminals of motor neurons [5]. Although vesicular

* Corresponding author. Fax: +1 203 785 7670.
E-mail address: leonard.kaczmarek@yale.edu (L.K. Kaczmarek).
[1] Present address: Bristol Myers-Squibb, Wallingford, CT 06492, USA.

0006-291X/$ - see front matter © 2007 Elsevier Inc. All rights reserved.
doi:10.1016/j.bbrc.2007.11.083

transport mechanisms could be different in the primate and rat, it is more likely that cellular regulation of this process differs in the two species.

Previous work has demonstrated that sodium pyrithione (NaP) elevates $[Ca^{2+}]_i$ in the bag cell neurons of *Aplysia* [6]. This elevation of $[Ca^{2+}]_i$ results from influx of calcium ions from the external medium, but it is not affected by blockage of voltage-gated Ca^{2+} channels. It is also unaffected by inhibition of voltage-gated Na^+ channels or a Na^+/K^+ ATPase inhibitor. The NaP-induced elevation of $[Ca^{2+}]_i$, was, however, attenuated by SKF 96365 and Ni^{2+}, two potential inhibitors of store-operated Ca^{2+} entry, suggesting that NaP activates a form of calcium influx in these invertebrate neurons.

In the present study, we have tested the effect of NaP on $[Ca^{2+}]_i$ in rodent and primate motor neurons to determine whether the mechanism underlying the elevation $[Ca^{2+}]_i$ is evolutionarily conserved and to determine whether there are any differences between the responses of these two types of neurons that may provide clues to differential behavioral sensitivity of the two species to NaP.

Materials and methods

Animals

Cultured embryonic rat spinal motor neurons were prepared as described by Fryer et al. [7]. For preparation of monkey neurons, rhesus monkey fetuses from time-mated pregnancies were delivered by cesarean section under isoflurane anesthesia. A total of two fetuses at embryonic days E37 and E56 were used in this study. Experiments were in strict accordance with the standards outlined in "Principles for Use of Animals and Guide for the Care and Use of Laboratory Animals." The protocol used in the rhesus studies was reviewed and approved by the Animal Care and Use Committee, University of Wisconsin.

Tissue preparations, cultures, and Ca^{2+} imaging

Rhesus motor neurons. Spinal cord tissues for cultures were prepared as described previously for monkey olfactory placode [8,9]. Briefly, fetal spinal cord (cervical, thoracic, and upper lumber region) was dissected out and thin coronal sections were made by a tissue chopper. The spinal cord of the older fetus was further halved at the midline. Two to three pieces of tissue were plated on a collagen or poly-L-lysine coated glass coverslip. Cultures on coverslips were maintained in 35-mm culture dishes containing growth medium (Medium 199, Gibco, Grand Island, NY) supplemented with 10% fetal bovine serum (HyClone, Logan, UT), 0.6% glucose, and 50 μg/ml gentamicin, and incubated at 37 °C with 1.5% CO_2 and 98.5% air. Medium was replaced every 3–4 days at the beginning of cultures and every 1–2 days after the cultures were established. Two to 4 weeks after spinal cord slices were grown in culture, they were loaded with 18 μM fura-PE3 acetoxy-methyl ester (Texas Fluorescence Labs Inc., Austin, TX) for 30 min in a 37 °C incubator. The indicator dye was dissolved in 2 ml of culture medium containing 0.05% BSA and 0.1% glucose (pH 7.4) with 6 μl of a solution made up of two parts DMSO and one part pluronic F-127 (BASF Corp., Parsippany, NY) by weight. After loading, cells were washed three times with culture medium and the photoengraved coverslips then mounted in a custom (Dvorak-Stotler) recording chamber, and placed on a Zeiss inverted microscope (ZM-135). Cells were continuously perfused at 50 μl/min with gassed (95% O_2 and 5% CO_2) culture medium or saline buffer at room temperature for 20 min before onset of recording. Ventral horn motor neurons were well labeled with fura and easily distinguished from other types of cells by their size (~8 μm diameter) and round shape with neurites. Approximately 30–50 motor neurons were viewed in an imaging field (750 × 750 μm) under 20× objective on each coverslip. Sequential 340/380 nm fura fluorescence excitation was achieved with a 75W Xenon lamp and filter wheel equipped with 340 and 380 nm excitation filters (see Fig. 1A). Pairs of 510 nm emission fluorescence were acquired every 30 s with a SIT video camera (Hamamatsu, Tokyo) attached to the epifluorescence port of the microscope. Metafluor software (Universal Imaging Corp., West Chester, PA) was used for acquisition and on-line display of the 340/380 fura excitation ratio. The ratio values were converted to $[Ca^{2+}]_i$ off-line as described below for rat neurons. At completion of imaging experiments the neurons in the recorded view were photographed and the photoengraved grid location was recorded for subsequent histological analysis of the cells in the field [9]. Neurons were then fixed in 2% paraformaldehyde (pH 7.6) for immunostaining.

Imaging of rat motor neurons. Neurons were placed on the recording chamber of a Nikon Diaphot inverted microscope equipped with a 40× objective [Nikon Plan Fluor Numerical Aperture (NA) = 1.3] or a 10× objective [Nikon Fluor (NA) = 0.5]. The Illumination system was a 75W Xenon arc lamp, coupled to the microscope via a fiber optic cable, and a computer-controlled grating/monochromator based excitation system (Photon Technology International, South Brunswick, NJ). Images were acquired with a Hamamatsu C2400 iCCD camera. The culture densities were such that 30–50 neurons were routinely monitored in a single field when using the 10× objective. Five hundred and ten nanometers of fluorescence emission images of a single field were sequentially acquired at 340 and 380 nm excitation wavelengths, and the acquisition time (including frame averaging when necessary) for a single full-frame (256 × 520 pixels) was 1–4 s. Ca^{2+} concentration sampling was performed at 30 or 60 s intervals. The camera gain voltage was set based on the initial fluorescence intensity of the cells at the beginning of each experiment and maintained constant thereafter. Between acquisition episodes the excitation illumination was blocked by automatic shutter control. Pixel/pixel intensity ratio images were converted to free $[Ca^{2+}]_i$ from the relationship $[Ca^{2+}]_i = Q * K_D * [(R - R_{min})/(R_{max} - R)]$ [10]. R_{min} and R_{max} were determined in intact motor neurons by applying 1–10 μM digitonin in Ca^{2+}-free buffer containing 0.5 mM EGTA, followed by perfusion with medium containing 2.3 mM Ca^{2+}. K_D is the dissociation constant of the fura-PE3/Ca^{2+} complex (250 nM). The constant Q was determined from the ratio of 380-nm evoked fura-PE3 fluorescence in 0 and 2.3 mM Ca^{2+}-containing buffer. Corrections for background fluorescence and camera dark current were carried out as described previously [11].

Identification of motor neurons. Motor neurons were identified as detailed in [9]. Briefly, once a recording experiment was complete, the imaged area was photographed and a coverslip grid reference was obtained to facilitate locating the cells after immunostaining. To identify motor neurons all coverslips were immunostained with the monoclonal antibody islet-1 39.4D5 (Santa Cruz, CA, 1:150 dilution), which recognizes islet-1 protein and 3,3′-diaminobenzidine (DAB) as the chromagen (Fig. 1). Some coverslips were double-stained with an antibody against neuron specific enolase (NSE, INCSTAR, Stillwater, MN, 1:1800) with another chromagen (Vector SG complex, Vector Lab, Burlingame, CA). Islet-1 immunopositive neurons were distinguished from other types of neurons and cells by their red-brown color and matched to the photographic and digitized fluorescence images that were acquired prior to immunostaining.

Results

As previously described for *Aplysia* neurons [6], exposure of isolated rat motor neurons to NaP in the presence of external Ca^{2+} stimulated Ca^{2+} entry that could be detected by imaging of intracellular Ca^{2+} using the ratiometric Ca^{2+} indicator dye fura-PE3 (Table 1). The NaP concentration that produces an increase in $[Ca^{2+}]_i$ that is 50% of the maximum response (EC_{50}) is 0.31 μM. The

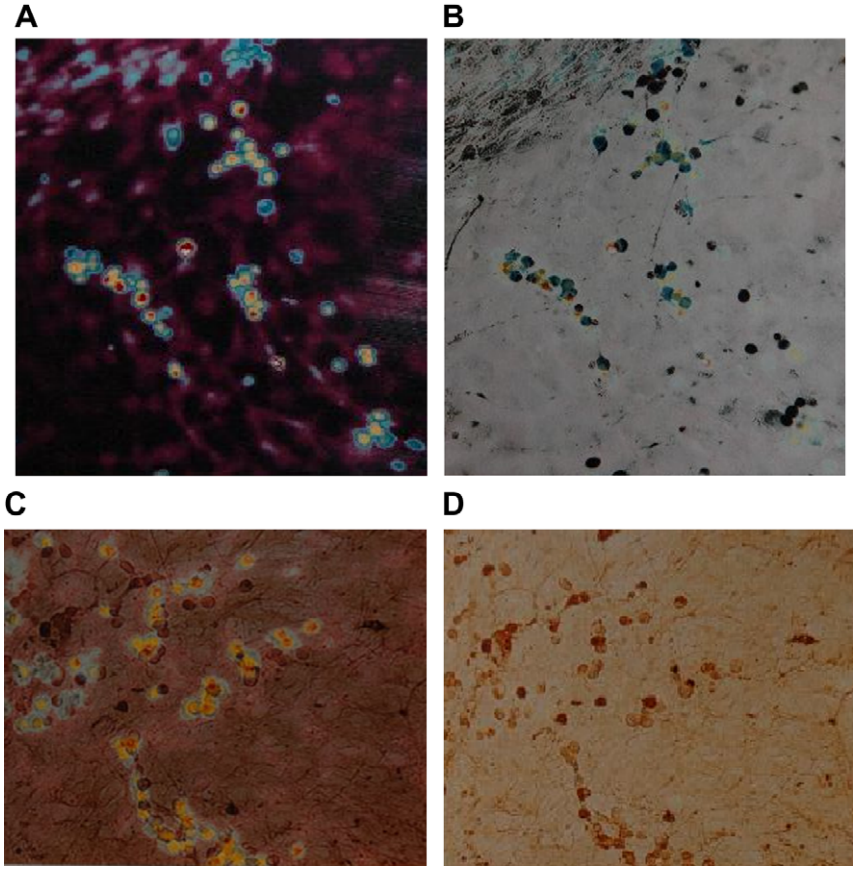

Fig. 1. Fura-PE3 and immunostaining images of rhesus ventral horn motoneurons. (A) Fura-PE3 image (380 nm excitation/510 nm emission) of rhesus ventral horn slice before addition of Na^+ pyrithione. Post Ca^{2+} imaging experiments motorneurons within the coverslip grid were identified by neuron specific islet-1 protein immunostaining using either monoclonal antibody islet-1 39.4D5 and 3,3′-diaminobenzidine (DAB) as the chromagen (brown cell bodies in (B) and (D)) or with an antibody against neuron specific enolase (blue cell bodies in (B)). (C) A digital overlay of a field stained with monoclonal antibody islet-1 39.4D5 and its corresponding pre-stimulated 380-nm Ca^{2+} image. Islet-1 immunopositive neurons were distinguished from other types of neurons and cells by their red-brown color and matched to the photographic and digitized fluorescence images that were acquired prior to immunostaining.

Table 1
Effect of Na on $[Ca^{2+}]_i$ (nM) in motor neurons from rat and monkey

Chemicals (Concentration)	Neuronal $[Ca^{2+}]_i$[a] (nM)	
	Rat	Monkey
NaP (μM)		
Negative control	90 ± 16	136 ± 30
0.043	101 ± 18	
0.10		138 ± 28
0.43	339 ± 17	
0.50		150 ± 23
1.0		159 ± 25
2.0		169 ± 30
4.3	426 ± 20	
10		202 ± 32
43	440 ± 22	
100		415 ± 39
200		386 ± 37

[a] Values for NaP represent means ± SD of data from 32 and 40 neurons in the rat and monkey, respectively.

NaP-induced Ca^{2+} entry was unaffected by nifedipine, a blocker of L-type voltage-dependent calcium channels or by tetrodotoxin, which blocks voltage-dependent sodium channels in nM concentrations. Calcium elevation was also unaffected by ouabain, an inhibitor of the plasma membrane Na^+–K^+ ATPase. Table 2 presents the effects of NaP on $[Ca^{2+}]_i$ in motor neurons alone or in combination with these pharmacological agents.

We also investigated the actions of SKF 96365, an antagonist of certain store-operated plasma membrane Ca^{2+} channels, that has previously been shown to block the actions of NaP in *Aplysia* neurons [6]. As in the latter cells, SKF 96365 inhibited NaP-evoked Ca^{2+} entry pathway in motor neurons, suggesting that the mechanism of action of NaP is conserved across species (Table 2).

NaP also produced an increase in $[Ca^{2+}]_i$ in motor neurons of the monkey (Table 1). As in the rat, this increase in the primate neurons was antagonized by SKF 96365 (Table 2). Quantitatively, however, there was a significant difference between these two species. The EC_{50} for the effect in motor neurons of the monkey was 10 μM, 30 times higher than observed in the rat, indicating that the rhesus motor neurons are apparently significantly less sensitive to the $[Ca^{2+}]_i$-elevating effect of NaP. The dose response relations for the rat and monkey motor neurons are compared in

Table 2
Effect of SKF 96365, tetrodotoxin, nifedipine or ouabain alone or in combination with NaP in rat motor neurons and of SKF 96365 alone or in combination with NaP in monkey motor neurons on neuronal $[Ca^{2+}]_i$ (nM)

Chemicals (Concentration)	Neuronal $[Ca^{2+}]_i$[a] (nM)	
	Rat	Monkey
SKF 96365 (20 μM)		
SKF 96365 (20 μM)	130 ± 14	158 ± 13
SKF 96365 (20 μM) + NaP (10 μM in rat and 100 μM in monkey)	162 ± 15	196 ± 11
Tetrodotoxin (1 μM)	128 ± 11	
Tetrodotoxin (1 μM) + NaP (10 μM)	237 ± 14	
Nifedipine (20 μM)	80 ± 10	
Nifedipine (20 μM) + NaP (10 μM)	216 ± 8	
Ouabain (1 mM)	117 ± 13	
Ouabain (1 mM) + NaP (10 μM)	302 ± 15	

[a] Each value represents means ± SD of data from 17 to 34 motor neurons in the rat and 39 motor neurons in the monkey.

Fig. 2, in which the data have been normalized to facilitate comparison of the two species. Motor neurons exhibited a concentration-dependent NaP-evoked increase in $[Ca^{2+}]_i$ that reached a plateau in both species. The onset of the NaP response was evident within 2–5 min, and reached peak levels between 15 and 25 min. Reversal of the effects, by switching to NaP-free solutions was only partially successful in the majority of cases. The dose–response curve for the Rhesus monkey motor neurons was, however, significantly shifted to the right compared to that of the rat, while the overall amplitude of the Ca^{2+} rise (3- to 4-fold over baseline) was similar in both species. The data also show that there is a clear threshold for the increase in $[Ca^{2+}]_i$ in the motor neurons from both species.

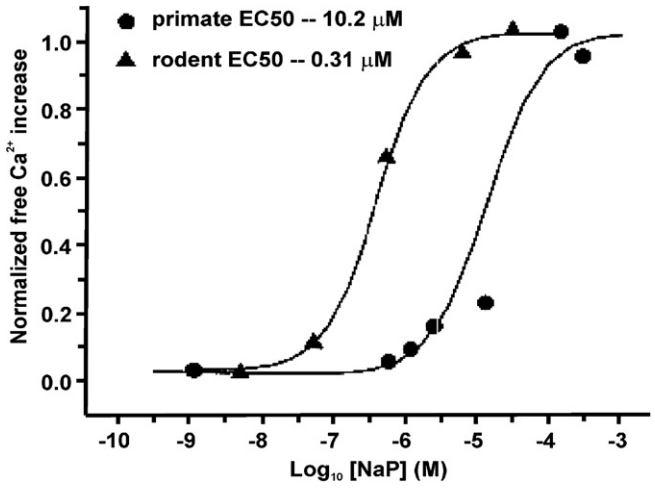

Fig. 2. Comparison of the increase in intracellular calcium concentration in rat and monkey motor neurons produced by sodium pyrithione. Data obtained from rat and rhesus motorneurons loaded with Fura-PE3, treated acutely with ascending concentrations of NaP, fit to a single-site logistic equation. The *y*-axis is the efficacy of the test concentration of NaP divided by the maximally effective concentration of NaP. Data points are the average from 32 to 40 neurons in the rat and monkey, respectively.

We also tested the effects of 2-methylsulfonylpyridine (2-MSP) on $[Ca^{2+}]_i$ in both rat and monkey motor neurons. This agent, which is the terminal serum metabolite in the pathway for ZnPt catabolism and fails to produce neurotoxicity *in vivo* in rats [12], was found to have no effect on Ca^{2+} entry in motor neurons of either species. 2-MSP is also the terminal serum metabolite for NaP since the first step in the catabolic sequence of ZnPt is free pyrithione [12], which is the dissociation product of NaP in aqueous solutions. In the rat neurons, basal $[Ca^{2+}]_i$ was 92 ± 22 nM and after treatment with 100 μM 2-MSP was 114 ± 21 nM ($n = 29$) while for the monkey neurons basal $[Ca^{2+}]_i$ was 158 ± 13 nM, and 176 ± 15 nM after exposure to 10 μM 2-MSP ($n = 44$).

Discussion

In resting neurons, the concentration of intracellular cytosolic Ca^{2+} is maintained at 50–200 nM. Transient increases in $[Ca^{2+}]_i$ provide control over physiological processes including modulation of ion channels, neurotransmitter release, and gene transcription [13]. An abnormally prolonged or large elevation in $[Ca^{2+}]_i$ is, however, associated with cellular processes leading to neuronal cell death [14–18]. The role of elevations of $[Ca^{2+}]_i$ in neuronal cell death has been studied in major part within the context of glutamate-mediated excitotoxicity [19].

We have found that, as reported for *Aplysia* neurons, NaP causes an elevation of $[Ca^{2+}]_i$ in rat and primate motor neurons. Although we investigated the actions of NaP, it is very likely that other formulations of pyrithione commonly used in proprietary preparations, namely ZnPt and the magnesium sulfate adduct of pyrithione disulfide, have the same cellular effects. In particular, ZnPt dissociates into two molecules of pyrithione in the rabbit during its absorption and distribution [20] and in the first step of its metabolism in rats, rabbits, dogs, and monkeys [12]. The magnesium sulfate adduct of pyrithione disulfide also undergoes cleavage to two molecules of pyrithione in the metabolic pathway leading to the terminal metabolite, 2-MSP [21]. 2-MSP is a metabolite of pyrithione in rats, rabbits, dogs, monkeys [12], and humans [22].

It is possible that a target of the NaP-induced $[Ca^{2+}]_i$ elevation in rodent neurons is axonal microtubules, which are responsible for axonal transport. Pyrithione, administered as ZnPt, has been shown to disrupt axonal flow in rat motor neurons. Repeated exposure of rats to ZnPt has been shown to reduce the rate of axoplasmic transport, and to lead to accumulation of tubulovesicular profiles at the distal nerve terminals [5]. An elevation of $[Ca^{2+}]_i$ of approximately 3-fold, similar to induced by NaP exposure, has been shown to influence the maintenance of microtubule integrity and axonal flow [23,24]. Exposure of neurons to the Ca^{2+} ionophore A23187 inhibits retrograde axonal transport [25], and interferes with assembly of microtubules [26]. Capsaicin elevates

$[Ca^{2+}]_i$ in somatosensory neurons by activating a Ca^{2}-permeable channel [27,28], and through its effects on $[Ca^{2+}]_i$ inhibits fast axoplasmic transport by disorganizing the axonal cytoskeleton [29]. Thapsigargin, a Ca^{2+}-ATPase inhibitor that promotes Ca^{2+} release from intracellular stores [30], can increase $[Ca^{2+}]_i$ by 2- to 3-fold [11] and inhibit fast axonal transport [31]. Moreover, cytoplasmic bleb formation occurs at a threshold of approximately 300–400 nM Ca^{2+} [18] and appears to involve disruption of cytoskeletal-membrane interactions. Thus, elevation of $[Ca^{2+}]_i$ by NaP may provide an explanation for the accumulation of tubulovesicular profiles within the terminals of rodent motor neurons following exposure to NaP *in vivo*.

The EC_{50} for the increase in $[Ca^{+2}]_i$ in the monkey motor neuron is 30 times that of the value in rats. Monkeys were administered NaP daily for 12 months [32] without developing neurotoxicity at a dose approximately 30 times higher than that shown to produce this effect in the rat [33]. Another pyrithione compound, the magnesium sulfate adduct of pyridine disulfide, also produces no detectable peripheral neuropathy in monkeys [21] at oral dose levels approximately 50 times the dose that produces this effect in rats. Monkeys did sustain sporadic emesis following dosing with pyrithiones, but this did not significantly influence absorption of a substantial portion of the dose. Based on the serum levels of 2-MSP in rats and monkeys following oral exposure, monkeys were systemically exposed to repeated doses of pyrithiones significantly higher than the doses that produce peripheral neuropathy in rats [21]. The concentration of 2-MSP in serum is proportional to the dose of pyrithione, thus it can be used as a measure of systemic exposure [12].

A recent study has demonstrated that ZnPt activates KCNQ2/Q3 potassium channels [34] in a reversible manner, and that this modulation is not mediated by Zn^{2+} ions, but is consistent with ZnPt binding directly to KCNQ channels. Interestingly, 20 mM NaP did not potentiate KCNQ currents, suggesting that the activation of Ca^{2+} entry observed in our studies is unlikely to be related to modulation of KCNQ channels.

In summary, our *in vitro* studies using motor neurons in the rat and monkey indicate that NaP, but not the terminal serum metabolite, 2-MSP, produces a rise in $[Ca^{2+}]_i$. The finding that the action of NaP is blocked by SKF 96365, an inhibitor of certain store-operated Ca^{2+} channels, suggests that NaP may, directly or indirectly, target such a channel, but future work will be needed to test this hypothesis. Although the results in rats and monkeys are qualitatively similar, a significant difference exists in the concentration of NaP that is required to produce an elevation of $[Ca^{2+}]_i$. In the primate, the threshold concentration and EC_{50} for the increase in $[Ca^{2+}]_i$ are significantly higher than those measured in rat motor neurons, suggesting that that this difference could underlie the observed differences in neurotoxicity between the two species.

Acknowledgments

This investigation was supported by National Institutes of Health grant NS 18492 to Yale University, National Institutes of Health grant P51RR000167 to Wisconsin National Primate Center, and a grant from Arch Chemicals to Yale University.

References

[1] J.F. Ross, G.T. Lawhorn, ZPT-related distal axonopathy: behavioral and electrophysiologic correlates in rats, Neurotoxicol. Teratol. 12 (1990) 153–159.
[2] D.R. Snyder, C.P. de Jesus, J. Towfighi, R.O. Jacoby, J.H. Wedig, Neurological, microscopic and enzyme-histochemical assessment of zinc pyrithione toxicity, Food Cosmet. Toxicol. 17 (1979) 651–660.
[3] C.S. Delahunt, R.B. Stebbins, J. Anderson, J. Bailey, The cause of blindness in dogs given hydroxypyridinethione, Toxicol. Appl. Pharmacol. 4 (1962) 286–291.
[4] A.B. Lansdown, Interspecies variations in response to topical application of selected zinc compounds, Food Chem. Toxicol. 29 (1991) 57–64.
[5] Z. Sahenk, J.R. Mendell, Axoplasmic transport in zinc pyridinethione neuropathy: evidence for an abnormality in distal turn-around, Brain Res. 186 (1980) 343–353.
[6] R.J. Knox, N.S. Magoski, D. Wing, S.J. Barbee, L.K. Kaczmarek, Activation of a calcium entry pathway by sodium pyrithione in the bag cell neurons of Aplysia, J. Neurobiol. 60 (2004) 411–423.
[7] H.J. Fryer, D.H. Wolf, R.J. Knox, S.M. Strittmatter, D. Pennica, R.M. O'Leary, D.S. Russell, R.G. Kalb, Brain-derived neurotrophic factor induces excitotoxic sensitivity in cultured embryonic rat spinal motor neurons through activation of the phosphatidylinositol 3-kinase pathway, J. Neurochem. 74 (2000) 582–595.
[8] E. Terasawa, C.D. Quanbeck, C.A. Schulz, A.J. Burich, L.L. Luchansky, P. Claude, A primary cell culture system of luteinizing hormone releasing hormone neurons derived from embryonic olfactory placode in the rhesus monkey, Endocrinology 133 (1993) 2379–2390.
[9] E. Terasawa, W.K. Schanhofer, K.L. Keen, L. Luchansky, Intracellular Ca(2+) oscillations in luteinizing hormone-releasing hormone neurons derived from the embryonic olfactory placode of the rhesus monkey, J. Neurosci. 19 (1999) 5898–5909.
[10] G. Grynkiewicz, M. Poenie, R.Y. Tsien, A new generation of calcium indicators with greatly improved fluorescent properties, J. Biol. Chem. 260 (1985) 3440–3448.
[11] R.J. Knox, E.A. Jonas, L.S. Kao, P.J. Smith, J.A. Connor, L.K. Kaczmarek, Ca2+ influx and activation of a cation current are coupled to intracellular Ca2+ release in peptidergic neurons of Aplysia californica, J. Physiol. 494 (Pt. 3) (1996) 627–639.
[12] W.B. Gibson, A.R. Jeffcoat, T.S. Turan, R.H. Wendt, P.F. Hughes, M.E. Twine, Zinc pyridinethione: serum metabolites of zinc pyridinethione in rabbits, rats, monkeys, and dogs after oral dosing, Toxicol. Appl. Pharmacol. 62 (1982) 237–250.
[13] I.B. Levitan, L.K. Kaczmarek, The Neuron, Oxford University Press, New York, 2002.
[14] D.R. Dowd, Calcium regulation of apoptosis, Adv. Second Messenger Phosphoprotein Res. 30 (1995) 255–280.
[15] D.J. McConkey, S. Orrenius, The role of calcium in the regulation of apoptosis, J. Leukoc. Biol. 59 (1996) 775–783.
[16] D.J. McConkey, S. Orrenius, The role of calcium in the regulation of apoptosis, Biochem. Biophys. Res. Commun. 239 (1997) 357–366.
[17] P. Nicotera, S. Orrenius, The role of calcium in apoptosis, Cell Calcium 23 (1998) 173–180.
[18] B.F. Trump, I.K. Berezesky, Calcium-mediated cell injury and cell death, FASEB J. 9 (1995) 219–228.

[19] J.M. Dubinsky, Examination of the role of calcium in neuronal death, Ann. N. Y. Acad. Sci. 679 (1993) 34–42.
[20] C.D. Klaassen, Absorption, distribution, and excretion of zinc pyridinethione in rabbits, Toxicol. Appl. Pharmacol. 35 (1976) 581–587.
[21] I. Bio/dynamics, A Six Month Oral Toxicity Study of Omadine-MDS (Magnesuim Sulfate Adduct of Pyrithione) in Monkeys. Technical Study Report. Project No. 80-2499. East Millstone, NJ, 1981.
[22] J.H. Wedig, S.J. Barbee, C. Mitoma, Pyrithione: plasma metabolite in man, Fundam. Appl. Toxicol. 4 (1984) 497–498.
[23] S.Y. Chan, S. Ochs, R.M. Worth, The requirement for calcium ions and the effect of other ions on axoplasmic transport in mammalian nerve, J. Physiol. 301 (1980) 477–504.
[24] M.P. Mattson, M.G. Engle, B. Rychlik, Effects of elevated intracellular calcium levels on the cytoskeleton and tau in cultured human cortical neurons, Mol. Chem. Neuropathol. 15 (1991) 117–142.
[25] G.J. Lees, Inhibition of the retrograde axonal transport of dopamine-beta-hydroxylase antibodies by the calcium ionophore A23187, Brain Res. 345 (1985) 62–67.
[26] E. Esquerro, A.G. Garcia, P. Sanchez-Garcia, The effects of the calcium ionophore, A23187, on the axoplasmic transport of dopamine beta-hydroxylase, Br. J. Pharmacol. 70 (1980) 375–381.
[27] K.E. Akerman, M. Gronblad, Intracellular free [Ca2+] and [Na+] in response to capsaicin in cultured dorsal root ganglion cells, Neurosci. Lett. 147 (1992) 13–15.
[28] P.S. Chard, D. Bleakman, J.R. Savidge, R.J. Miller, Capsaicin-induced neurotoxicity in cultured dorsal root ganglion neurons: involvement of calcium-activated proteases, Neuroscience 65 (1995) 1099–1108.
[29] T. Kawakami, N. Hikawa, T. Kusakabe, M. Kano, Y. Bandou, H. Gotoh, T. Takenaka, Mechanism of inhibitory action of capsaicin on particulate axoplasmic transport in sensory neurons in culture, J. Neurobiol. 24 (1993) 545–551.
[30] O. Thastrup, P.J. Cullen, B.K. Drobak, M.R. Hanley, A.P. Dawson, Thapsigargin, a tumor promoter, discharges intracellular Ca2+ stores by specific inhibition of the endoplasmic reticulum Ca2(+)-ATPase, Proc. Natl. Acad. Sci. USA 87 (1990) 2466–2470.
[31] R. Hammerschlag, Is the intrasomal phase of fast axonal transport driven by oscillations of intracellular calcium? Neurochem. Res. 19 (1994) 1431–1437.
[32] International Research and Development Corporation, One Year Oral Toxicity Study in Cynomolgus Monkeys using Sodium Pyrithione. Technical Study Report. Study Number 397-047. Mattawan, MI, 1989.
[33] Toxicol Laboratories, Ltd., Subchronic (90-day oral gavage) study in the rat using sodium pyrithione. Report No. OLA/2/88. Ledbury, England, 1988.
[34] Q. Xiong, H. Sun, M. Li, Zinc pyrithione-mediated activation of voltage-gated KCNQ potassium channels rescues epileptogenic mutants, Nat. Chem. Biol. 3 (2007) 287–296.